

Received June 14, 2020, accepted July 1, 2020, date of publication July 7, 2020, date of current version July 20, 2020.

Digital Object Identifier 10.1109/ACCESS.2020.3007615

# Speed Control of Direct Current Motor Using ANFIS Based Hybrid P-I-D Configuration Controller

YANLING GUO AND MOHAMED ELHAJ AHMED MOHAMED<sup>ID</sup>, (Member, IEEE)

Mechanical and Electrical Engineering College, Northeast Forestry University, Harbin 150040, China

Corresponding author: Mohamed Elhaj Ahmed Mohamed (mohaj2007@hotmail.com)

This work was supported in part by the Natural Science Foundation of Heilongjiang Province under Grant ZD2017009, and in part by the National Key R&D Program of China under Grant number 2017YFD0601004.

**ABSTRACT** Considering DC motor's non-linear characteristics, design challenges and mechanical variation due to the operation conditions, the precise controller cannot be performed using the traditional control alone. This study presents an innovative method to optimize the direct current motor speed by decreasing the transient response characteristics such as overshoot, settling time and rise time. In this study, several PID's configurations and ANFIS controllers have been performed for direct current motor speed control. The suggested techniques were compared to each other to validate the superiority of the highest controller performance. Training data for ANFIS was generated using standard configuration, cascade and dual configuration. The dual configuration is a hybrid of two controller's data manipulated using a special algorithm. The results obtained using Matlab Simulink tools demonstrated the efficiency of ANFIS based dual PID and ANFIS based PD methods for controlling the motor speed. The overall simulation results showed that the models have a rapid response, small overshoot, superior dynamics and robustness, and static performance. The techniques presented herein outperform the traditional control methods for obtaining highly accurate control.

**INDEX TERMS** ANFIS, direct current motor, PID, PI, PD, feedforward data and algorithm.

## I. INTRODUCTION

The primary purpose of control is to allow the model to operate reliably and enhance its performance. This goal can be achieved by implementing the engineering concepts to control the process. Direct current motor speed control means adjusting the speed to the required value to realize a given operation. Thus, each direct current motor requires a controller to adjust its direction or the speed to the desired value. In most cases, the control performs manually (by hand) or by applying some traditional/intelligent control techniques. The motor produces the most needed mechanical motion, which is categorized into direct current and alternate current motors. Indeed, motors commonly used to convert the direct or alternating current to mechanical energy has been implemented in several applications and equipments. The increased precision and accurate motor movement dynamic has resulted in widespread use of high performance direct current motors.

Regulation of the DC motor speed is essential as it allows the generation of an accurate and precise speed. Previous

studies have presented several controllers to enhance the performance of the DC motor. PID control is the most suitable technique for industrial application, but it requires an accurate mathematical model for the control system [1]–[3]. The essential concept for designing a PID controller includes tuning of the P, I, and D gains. This may also include several other tuning manual methods such as those in the industrial field manual. Furthermore, some methods are a combination of intelligent methods such as ANFIS, Fuzzy control, computation algorithms, and neural network [4]–[8]. During the operation, the disturbance and changing of the parameters can destabilize the system. Due to the recent increase in the system's complexity, there are often challenges when tuning the PID's parameters to obtain perfect transient characteristics and stable systems. Therefore, control designers have switched to intelligent strategies to obtain optimal performance [9], [10].

As mentioned, control designers have applied intelligent techniques to avoid drawbacks related to the traditional method. Fuzzy control is one of the modern methods applied to enhance the control of the DC motor. Recently, an advanced technique for tuning scale factor of Fuzzy

The associate editor coordinating the review of this manuscript and approving it for publication was Ting Yang<sup>ID</sup>.

PD-I model combined with anti-windup was developed to avoid the overall gain of the model and limiting of the oscillatory in the controlled variables [11]. Model-reference adaptive fuzzy was recommended for the control of the DC motor's speed; the controller required a reference model for training FIS, and an oscillation appeared in the speed response [12]. On the other hand, due to the rapid development in the application, several studies have used fuzzy logic combined with ANFIS to improve control efficiency. In [13], fuzzy-based PID online supervised adaptive network FIS based was introduced for controlling the DC motor speed, obtained results using Simulink toolkits showed perfect performance in transient response characteristics. ANFIS has been used to regulate the speed of the DC motor, and the efficiency was compared to the traditional PI controller and fuzzy-based PID control [14]. Although the controllers used in the comparison showed excellent performance in settling time and rise time, there was a significant overshoot and small steady-state error.

ANFIS, as a modern technique, has replaced traditional methods in many applications. In order to decrease the transient response parameters such as the overshoot, rise time and settling time for SEDC motor, an intelligent control based ANFIS has been proposed. Simulation results have demonstrated suitable rise time and sustainable overshoot with oscillation before reaching the steady-state [14]. On the other hand, different researchers have applied trained feed-forward of ANFIS based on several algorithms. Premkumar introduced ANFIS online-based GA-PSO optimized BLDC motor speed control has been by using a hybrid algorithm [15], while other studies [16], [17] introduced ANFIS based rotor position control for DC motor. A novel bacterial Foraging PSO and BAT, ANFIS Optimization Algorithms based speed control has been introduced to (MC)-fed brushless dc motor, where the results proved superior performance to other techniques under various operation conditions [18].

Generating data for training ANFIS is an essential aspect of designing the ANFIS controller [19]. In [20] fractional-order PID was designed with the GA algorithm to train ANFIS data where three ANFIS configurations were formed using training data to tune the parameters during the operation. In other studies, speed control based ANFIS was developed using three layers backpropagation algorithm [22]. In this model, the parameters measured only focused on the rise time and the settling time, which both showed high values for the designed controller and controllers introduced for comparing the performance [22]. Moreover, ANFIS based PSO and recursive-least-square has been used for DC motor speed controller as multi-level ANFIS, and the method provides optimal performance [21]. For the ANFIS and PI-based MPPT algorithm controllers presented for control BLDC motor speed, the performance of the designed method was evaluated by comparing to the observed method. The suggested controller showed its feasibility and suitability under different situation [22].

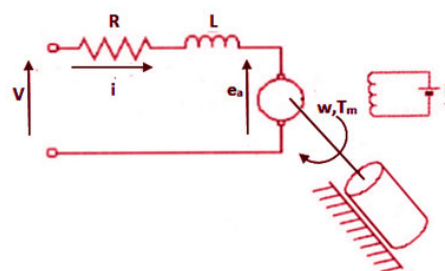


FIGURE 1. DC motor equivalent circuit.

Having considered the points outlined above, various studies on the control of the speed of DC motors have been conducted. The studies demonstrate how fuzzy logic control and ANFIS control can provide suitable methodologies to determine the best control. Meanwhile, DC motor speed could be regulated using several techniques. In this regard, most of the previous studies have some drawbacks. For instance, their main goal is to minimize the transient response parameters, but there are often deviations from this goal, and there are significant similarities in most techniques used. In order to avoid these inefficiencies; this work presents the speed control of the DC motor by controlling the armature voltage. In this method, the control is done using ANFIS based on several PIDs forms as a controller for the DC motor. The PID model design is used as a basis to prepare training data of the proposed controllers. For comparison purposes, the DC motor model was operated using designed controllers. Furthermore, the simulation model was performed repeatedly to meet different conditions, including sudden change of the speed values or change in the input signal characteristics. The efficiency of the suggested controllers were validated using various kinds of speed signals. This study aims at implementing cascade and dual block to control the DC motor speed.

This paper is organized as follows: The second section describes the mathematical model of the DC motor, and all relevant mathematical equations have been detailed. Part three of this paper discusses the introduced controllers, while part four illustrates the results and curves attained by introduced controllers using Matlab toolkits. Finally, the conclusions drawn from this study are shown in part five.

## II. MOTOR MODEL

DC motor used for this study is separately-excited and has the ability to separately control over the speed and torque by regulating the field current and armature current. According to figure 1, the developed torque is illustrated using equation 1 and 2, where the armature current is  $I(t)$ , angular speed is  $\omega$ , interior friction is  $J$ ; the friction coefficient is  $\beta$ , and torque constant is  $k_a$ . Armature voltage  $e(t)$  is given by equation 3, where  $K_b$  Back emf constant, an applied voltage is symbolized by  $V(t)$  and can be calculated using equation 4.  $L$  represents the Armature inductance, whereas  $R$  represents resistance. Equation 5 explains the motor

TABLE 1. The parameters of the DC MOTR.

Parameter	Value
Armature inductance L	0.005 H
Armature resistance R	0.1 Ω
Rotor inertia J	0.1 N.m2
Viscous friction coefficient B	0.05 Nms/rad
Back emf constant $K_b$	0.004Vs/rad
Torque constant $K_a$	0.0036 Nm/A

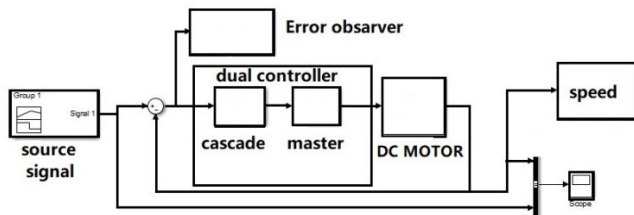


FIGURE 2. The model used to produce training data for the dual controller.

transfer function. Table1 describes the parameters of the dc motor.

$$T(t) = J \cdot \frac{d\omega(t)}{dt} + B \cdot \omega(t)$$

$$T(t) = K_a \cdot i(t)$$

$$e_a(t) = K_a \cdot \omega(t)$$

$$v(t) = L \cdot \frac{di(t)}{dt} + R_i(t) \cdot e_a(t)$$

$$\frac{\omega(s)}{v(s)} = \frac{K_a}{k_a k_b + (Js + B) + (Ls + R)}$$

### III. PROPOSED CONTROL TECHNIQUE

To produce suitable training data for ANFIS controller, this study was conducted in many PIDs configurations to prove the perfect configuration for training ANFIS. The configurations implemented the PI, PD and PID. Cascade compensated for previous controllers which we were labelled as dual PI, dual PD and dual PID. The dual-controller was then manipulated using an algorithm to conduct the convergence and divergence among the two models.

In this stage, the DC motor function was operated under different controllers. The linearization Continuous-time transfer function of the dc motor used to apply the control was as follows:

$$7.2$$

$$\frac{1}{s^2 + 20.5s + 10.03}$$

In this strategy, the PIDs configurations were used to generate training data for ANFIS control. The DC motor was controlled by several ANFIS controllers based on different PIDs forms. The first controller was ANFIS based PID. The model used to produce training data for the dual controller is illustrated in figure 2.

TABLE 2. The transfer functions of suggested controllers.

Configuration transfer function	First configuration
PI	$10.24s + 5.601$
PD	$\frac{7.598e05s + 1.704e07}{s + 2.502e04}$
PID	$\frac{326.1s^2 + 7762s + 5345}{s^2 + 850.9s}$

TABLE 3. The transfer functions of suggested controllers.

Configuration transfer function	Cascade configuration
PI	$3.888s + 0.8321$
PD	$\frac{1.893s + 169.3}{s + 100}$
PID	$\frac{2.139e07s^2 + 1.378e10s + 1.807e12}{s^2 + 2.395e06s}$

The PIDs controllers were used to generate training data for ANFIS configuration. The DC motor was controlled by several ANFIS controllers based on different PIDs forms. The first controller was ANFIS based PID. The transfer function of the first PID controller, as well as the PID<sub>2</sub> designed to work with the PID<sub>1</sub>, are explained in tables 2 and 3. The PID<sub>2</sub> cannot provide a high performance for the control of the DC motor transfer function but only clarifies the controller Strict. The controller transfer function was listed in table 3. The PID<sub>2</sub> controller was built based on the parameters, as illustrated in figure 9. In the last step, the two PIDs merged to form the dual PID controller, which showed a high performance, although the dynamic was still too slow. The function of the dual PID controller is described in table 4. For the slow speed of the controller response, a controller was implemented to create data for training ANFIS model to solve the problem of the response speed. However, the data generated was too big, and the extracted data was therefore minimized in order to increase the controller speed response, leading to high performance.

The artificial neural network is a new control strategy, which manipulates the numerical entities to perform the divergence and convergence among them. The incorporation of fuzzy and neural network produced a modern method that gained the features of both strategies and resulted in a significant improvement in nonlinear mapping, modelling, learning and pattern realization. In this context, several models are designed to generate ANFIS training data and to demonstrate

**TABLE 4. The transfer functions of suggested controllers.**

Configur- ation transfer function	Dual configuration
PI	$\frac{39.8 s^2 + 30.3 s + 4.661}{s^2}$
PD	$\frac{1.438e06 s^2 + 1.609e08 s + 2.885e09}{s^2 + 2.512e04 s + 2.502e06}$
PID	$\frac{6.975e09 s^4 + 4.658e12 s^3 + 6.963e14 s^2 + 1.41e16 s + 9.659e15}{s^4 + 2.396e06 s^3 + 2.038e09 s^2}$

the impact of the data in the performance of the controller. The models that have been built are commonly known as the PI, PD and the PID. Moreover, new forms of PIDs have been presented, such as dual PI, dual PD and dual PID. Each dual-block is a hybrid of the two configurations, which were later manipulated using the convergence and divergence algorithm, as explained in the flowchart in figure4.

The efficiency of standard configurations is predictable, but the performance of the newly presented methods might be more optimized. By observing the motor behaviour, the data was generated and loaded in the neuro-fuzzy designer. FIS was created based on the grid partition with function two inputs (linear type- each one is four triangle membership function). The optimization method for training the FIS data was back propagation with error tolerance zero and epoch 10, and the data was subsequently tested for error. ANFIS in this method was implemented using 53 nodes, and the total number of parameters was 16 linear parameters and 24 nonlinear parameters. The number of data pairs were then checked using the 16 fuzzy rules, and by adjusting the inputs rules to get an optimal response.

The numerical entities were loaded in FIS to track the I/O for the provided data, and on-line was performed to identify the objects during the operation, which needs the neuron network structure suitable for the learning strategy. The most important factor is the speed of the learning mechanism, and if the configuration is too complicated it could affect the adapting speed, making it difficult to trace the objects. For all the suggested controllers, an FIS based Takagi-Sugeno model performed an ANFIS configuration with two inputs, where one output was later utilized as a control signal [23].

Design of (ANFIS) controller is the most approved intelligent controls strategies [24]. ANFIS is a combination of Fuzzy logic, and neural network, both of them have some components and objectives. Both techniques attempt to figure out the functioning of human knowledge. In both methods, the theorem is to store the expert’s knowledge to make a suitable decision. In essence, adaptive neural fuzzy is a kind of fuzzy logic enhanced by a neural network to develop

the performance of the control [25].ANFIS is fuzzy rules enhanced by a neural network to carry out the system behavior based on I/O data. The combination of these intelligent strategies hybridizes the Takagi–Sugeno with the learning capabilities. The learning process role is to regulate the fuzzy inference system parameters.

The main objective of ANFIS is to implement the configuration of a neural network to develop the process of fuzzy parameters to represent the neuron’s weight.. Therefore, ANFIS can automatically recognize by regulating the MF and modifying the neural-network weight using a suitable algorithm. As a consequence, the neural network architecture can be optimizing the membership function, since the fuzzy configuration built based three parts, fuzzy input, inference mechanism, which is known as fuzzy rules and the output of the system, where several techniques can implement all these parts. Usually, ANFIS uses Takagi–Sugeno, where it is applicable in controlling and modelling complicated process. In this design of this controller as presented in figure 2, this structure mainly contains five layers which are rule base, database, decision unit, fuzzification and defuzzification unit. ANFIS’s every layer is corresponding to the Takagi Sugeno FIS[26, 27].

The flowchart of the algorithm, as in figure 4, is describing all steps of manipulating data generated to train the ANFIS controller. The algorithm established, three groups (i, k, j) were initially were set to zero = 0 for use as index and counter, where (i) and (j) are the data set of two controllers (cascade controller and master controller), and (k) is the new hybrid data set (dual controller). The variables  $A_k, B_k, U_k, S_k, R_k$  are defined.  $U_k$  was used to set the intersection between two inputs that represent the data in  $A_k$  and  $B_k$ , where they were symbolled in the algorithm as ( $U_k = (A_k \cap B_k)$ ).  $S_k$  was used to set out the symmetric difference among the two data sets, and it was represented in the algorithm as  $S_k = \{j:(j \in A_k) \text{ or } (j \in B_k)\}$ . The variable  $R_k$  was used to carry the union of the two data items ( $R_k = U_k \cup S_k$ ). The counter k increased until the completion of the criterion.

In this controller, ANFIS are extracted using models explained previously in tables 2, 3 and 4, where the double controller has implemented previously and as PIPD and proved a good performance [19].In the ANFIS process, firstly the training data is loaded from the model used to generate it. It is secondly converting this training data to fuzzy set form based on suitable member function; this step called fuzzification and membership function selection. Then creating a fuzzy rule frame(if-the-else)corresponding to the fuzzified input weight. Fourth, updating the parameters using the training data algorithm based on error tolerance. In the final step, which is a defuzzification step, the fuzzified data will be reorganized as numerical data to run as an ANFIS model.

By considering a fuzzy inference system with two inputs (x, y), and one output (f), The rule base should be created with two Takagi–Sugeno fuzzy rules type [22].ANFIS rules form based on Takagi–Sugeno is given as in equations below,

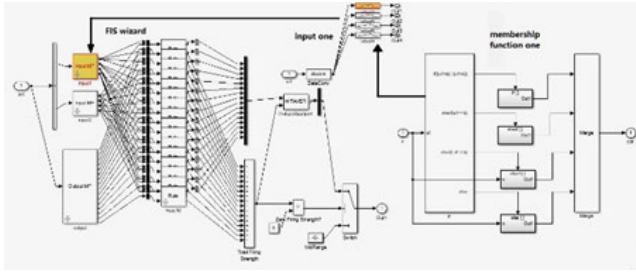


FIGURE 3. The architecture of ANFIS network.

Rule 1: If  $X$  is  $A_1$  and  $y$  is  $B_1$ , then

$$f_1 = p_1x + q_1y + r_1;$$

Rule 2: If  $X$  is  $A_2$  and  $y$  is  $B_2$ , then

$$f_2 = p_2x + q_2y + r_2;$$

where fuzzy antecedent sets  $A_1, A_2, B_1$  and  $B_2$  are the consequent crisp function.  $Fz$  is the output resulted by rule  $z, p_z, q_z$  and  $r_z$  are the parameters resulted by rule  $z$ . Layer1 has  $N$  nodes; these nodes numbers are equal to the variables number of that transmitted data to each node of the next layer. Each neuron in this layer uses its transfer function to calculate a certain degree of a specific fuzzy subset. In this layer executing the fuzzification strategy to carry out the output according to the equation below,

$$o_i^1 = \mu_{A_1}(x) = \frac{1}{1 + \left( \left( \frac{x - c_1}{a_1} \right)^2 \right)^{b_1}}$$

where the parameters  $a$  and  $c$  using to modify the MF shape.

ANFIS model has two inputs with four trmf and one linear output type. 16 FIS rules were implemented. The FIS was optimized using backpropagation for training the numerical entities. According to previous factors, the implemented neural network was as demonstrated in figure 3.

The second layer of ANFIS controller is calculating the MF and the weight factor values using explained equation below, which is presenting the fuzzy-sets, where each neuron is a rule premise.

$$w_i = \mu_{A_1}(x) * \mu_{B_1}(y)$$

The normalization of the relation between the fuzzy inputs and realizing of fuzzy operation it is the responsibility of the third layer.

$$\bar{w}_i = \frac{w_i}{w_1 + w_2} \quad (i = 1, 2)$$

In the fourth layer, the nodes compensate for the operation and execute the rules of the fuzzy system. The output of this layer has explained in equation below.

$$o_i^4 = \bar{w}_i * f_i = \bar{w}_i * (p_1x + q_1y + r)$$

The defuzzification process is performed in the fifth layer, where all input signals summation are summed in this layer

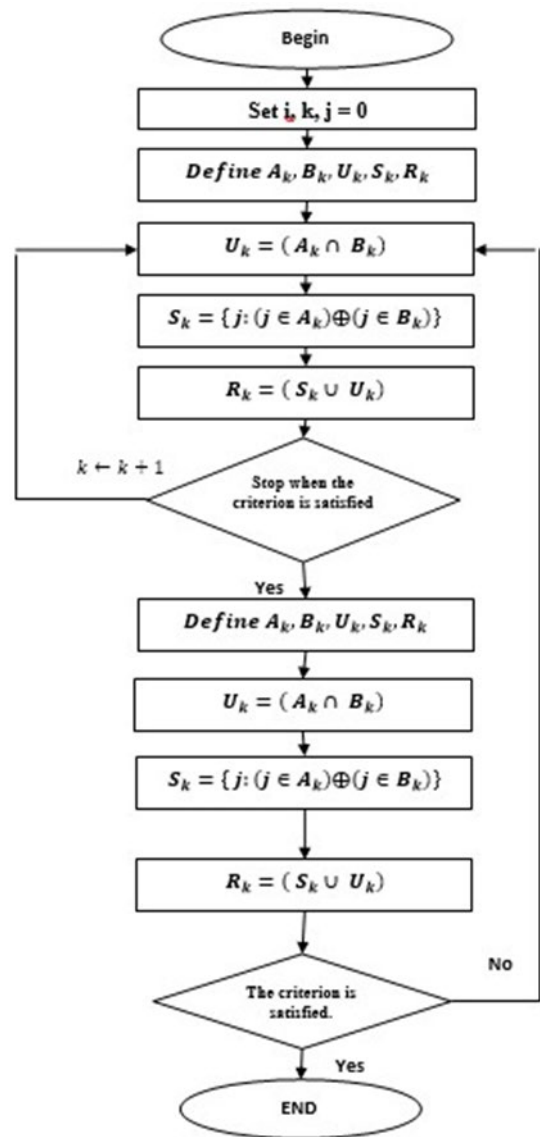


FIGURE 4. The algorithm of convergence and divergence.

as explained in the equation below.

$$o_i^5 = \sum_i \bar{w}_i * f_i = \frac{\sum_i \bar{w}_i * f_i}{\sum_i \bar{w}_{ii}}$$

The suggested controllers were adjusted correctly and investigated to ensure their efficiency. They were also validated to make the data set output predictable. In order to increase the speed of the dynamic response, generated data was minimized to the size that is able to gain the target. The models were operated using different input signals and speed in order to increase the efficiency. An optimal controller was obtained through several modifications of the error tolerance, membership functions and optimization methods. The schemes used to perform ANFIS based dual PID are demonstrated in figures 5 and 6, respectively. Figure 7 demonstrates the Simulink model ANFIS dual controller.



FIGURE 5. Dual PID training errors for ANFIS.

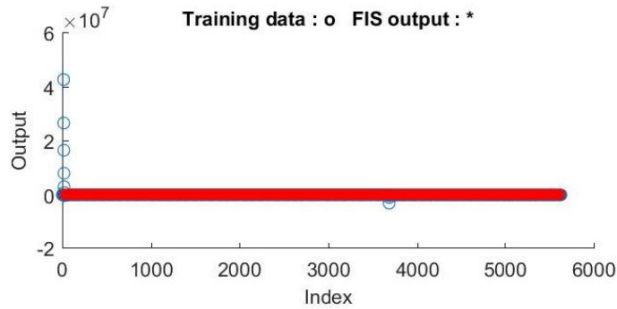


FIGURE 6. Dual PID training data for ANFIS.

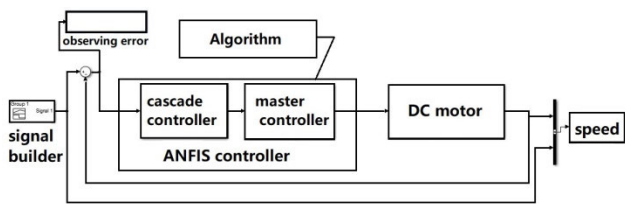


FIGURE 7. The Simulink model ANFIS dual controller.

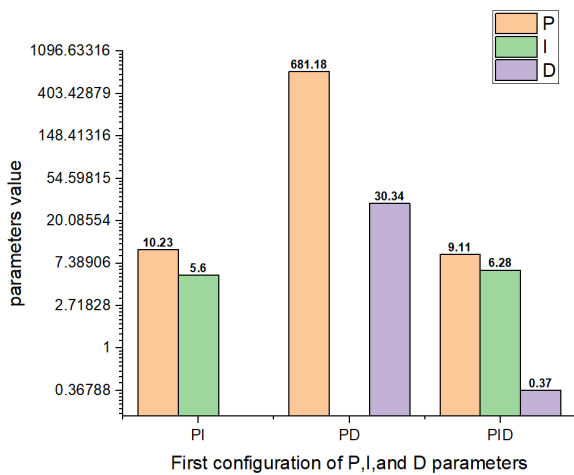


FIGURE 8. The parameters of the first configuration.

For the PI controller, similar procedures of PID were followed. First, the DC motor function was tuned using  $PI_1$  controller, and the TF is illustrated in table 2. The controller was adjusted to the parameters, which is illustrated in figure 8. For the  $PI_2$  controller, the transfer function is shown in table 3, and the parameters are demonstrated in figure 9. Designing of the dual PI controller achieved using the parameters is

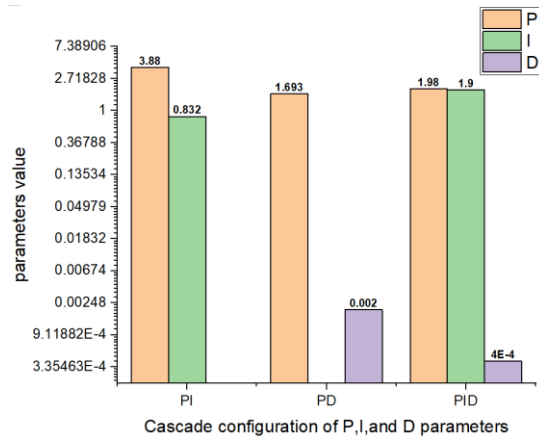


FIGURE 9. The parameters of the cascade configuration.

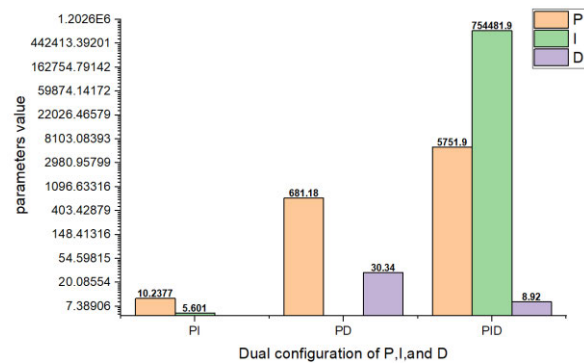


FIGURE 10. The parameters of the dual configuration.

demonstrated in table 4. The transfer function of the  $PI_2$  controllers are shown in figure 9. For the dual controller's blocks, no warnings or incompatibilities were identified in the linearization, and each block was accurately linearized. The dual PI controllers were tuned to the parameters as in figure 10.

Similar steps were repeated for the PD controller to confirm the performance effect of the dual control. The  $PD_1$  controller was implemented with the transfer function as shown in table 2. The controller was tuned to the P and D action, which were obtained, as explained in figure 8. The  $PD_2$  controller transfer function only used the proportional action because when the dual PD utilized the double derivative action, the system became unstable, and the transfer function is shown in table 3. The derivative action was minimized as low as possible. The specifications of the  $PD_2$  are illustrated in figure 9. For the dual PD that was operated as in previous controllers, the transfer function of the dual PD controller is illustrated in table 4. The parameters obtained using the dual PD controller are shown in figure 10.

#### IV. RESULTS AND DISCUSSION

First, the dc motor was operated without control to determine the effect of the control and the response showed inefficiency and sizeable steady-state error (Figure 11).

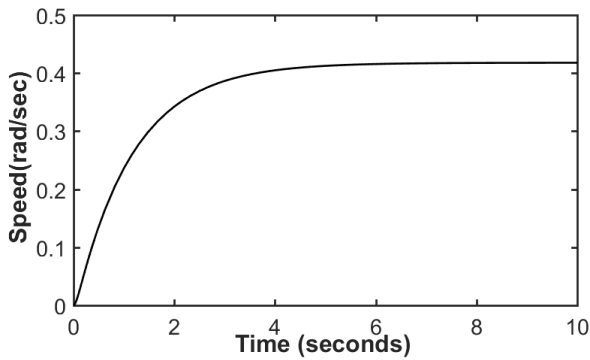


FIGURE 11. The step response of the dc motor function without control.

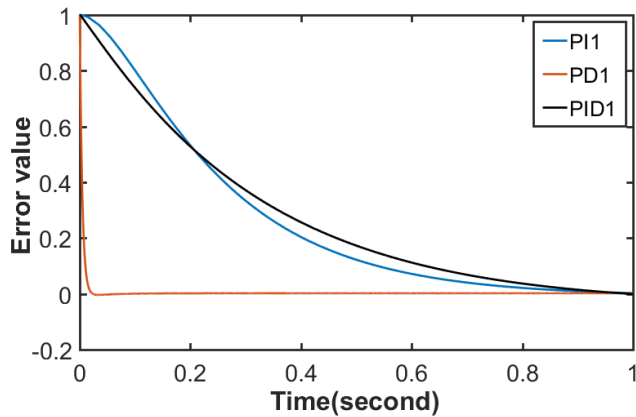


FIGURE 12. The error rate of three ANFIS configurations based  $PI_1$ ,  $PD_1$ , and  $PID_1$ .

In this study, the error for each controller was measured and the motor behavior observed in order to retune the controller and generate suitable data for training ANFIS and subsequently ensuring optimal performance. For ANFIS based  $PI_1$  and  $PID_1$ , a significant error was observed because the controllers adjusted to maximum performance and were capable of working with the second controller. For the ANFIS based  $PD_1$  reaction, the controller showed minimum error. The error response of the three controllers is illustrated in figure 12.

The cascade configuration's controllers were operated separately from the master controllers, for the cascade ANFIS based  $PI_2$  and  $PD_2$ , the significant error was generated by these controllers in the error response (Figure 13).

The second  $PID_2$  controller showed the error produced by the  $PID_2$  without the master  $PID$  (Figure 14).

In the last level of tracking, an error was generated for the dual controllers, as shown in figure 15.

After controlling the DC motor speed using ANFIS based  $PID_1$  controller, the response was different from that of the input signal, but after repeated tests, there was improved performance, making it suitable for controlling again with the  $PID_2$  controller. Figure 16 shows the controller response. The transient parameters of the controller are explained in table 3 and figure 22. Figure 16 also demonstrates the dc motor speed response of the first ANFIS based  $PI_1$  AND  $PD_1$  controllers, where the  $PD_1$  controller demonstrated

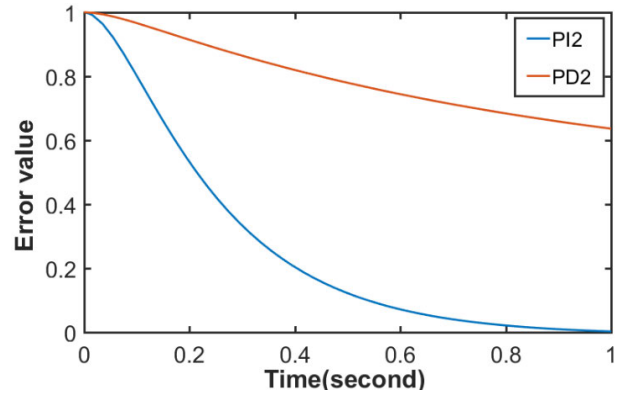


FIGURE 13. Error produced by the cascade  $PI_2$  and  $PD_2$ .

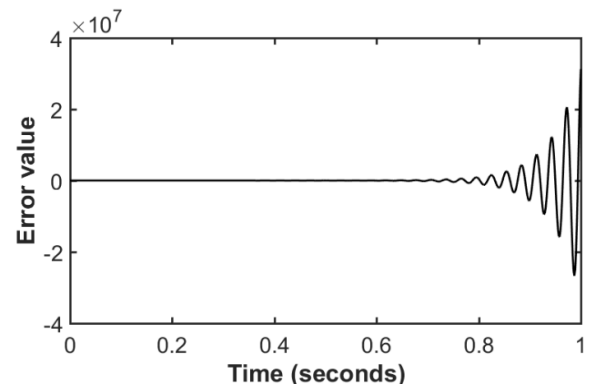


FIGURE 14. Error produced by the cascade  $PID_2$ .

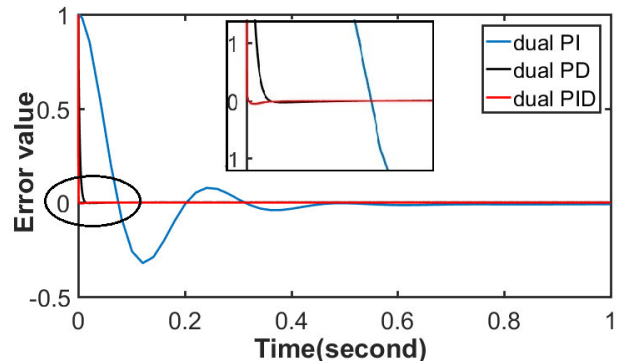


FIGURE 15. Error produced by the dual controllers.

better performance. For the ANFIS based  $PI_1$  as  $PID_1$ , the speed response showed a delay in settling time and rise time. The transient parameters were listed in table 3 and figure 22.

In the next operation, the dc motor control performance was evaluated using the cascade controller, which was subsequently termed as the second controller. Figure 17 shows the response of the ANFIS based  $PID_2$  separated from the  $PID_1$ , while table 5 and figure 22 show the transient parameters of the  $PID_2$  controller. The controller was built to support the first one, so the response was quite different from the desired speed.

With respect to the ANFIS based, the  $PI_2$  controller alone showed a varied response to the step input signal (figure18).

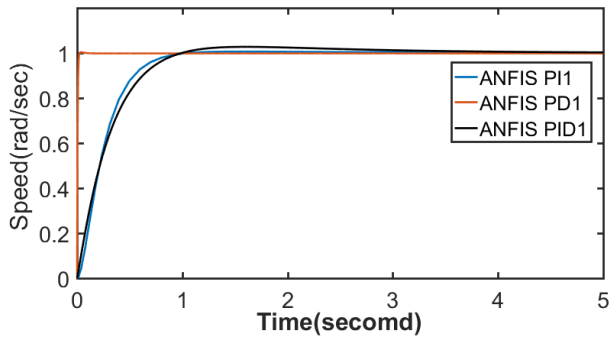


FIGURE 16. The speed response of the ANFIS controller-based  $PI_1$ ,  $PD_1$ , and  $PID_1$ .

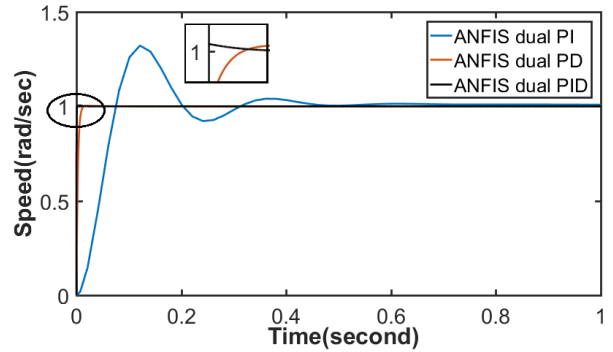


FIGURE 19. Speed response using ANFIS based dual PI, PD and PID.

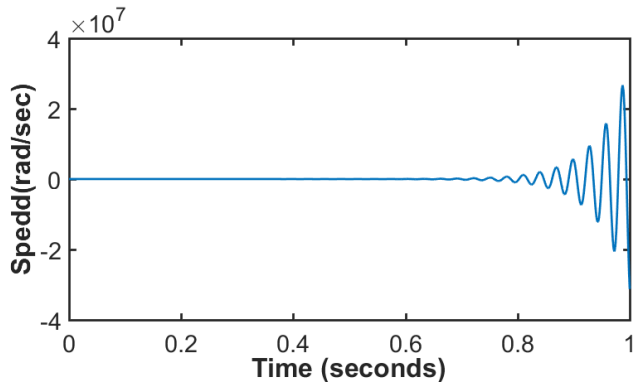


FIGURE 17. The response of the ANFIS based  $PID_2$ .

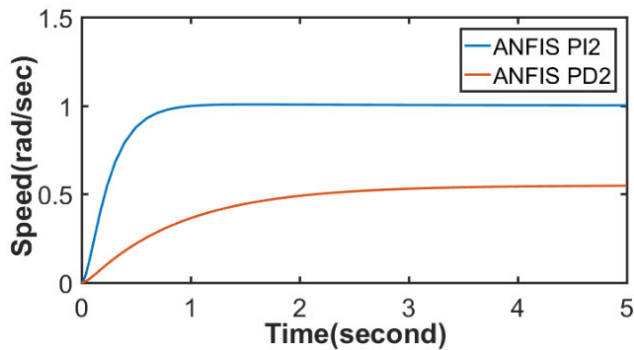


FIGURE 18. Speed response using ANFIS based  $PI_2$  and  $PD_2$ .

The response was as a result of using the  $PI_2$  controller far from the ideal response, but the objective of the controller is to work with the  $PI_1$  controller. The P and I action is a suitable asset value and can be achieved after repeating the tests many times. For the ANFIS based,  $PD_2$  controller transfer function only used the proportional action because in case of utilizing double derivative action. It made the system unstable, so the transfer function is  $P=1.693$ , and the derivative action minimized as small as possible. The effect of the  $PD_2$  alone was shown in table 5 and figure 22, while figure 18 illustrates the response of the ANFIS based  $PD_2$  controller.

Finally, the two controllers, i.e. the master and cascade were merged. For ANFIS based dual PID. The controller showed high performance. The ANFIS based dual PID

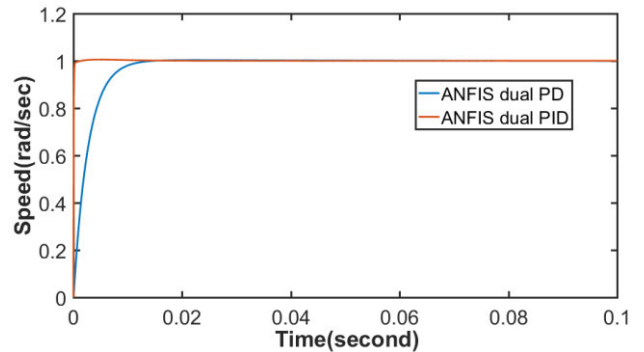


FIGURE 20. Speed response using ANFIS based dual PD and PID in the range 0.1 second.

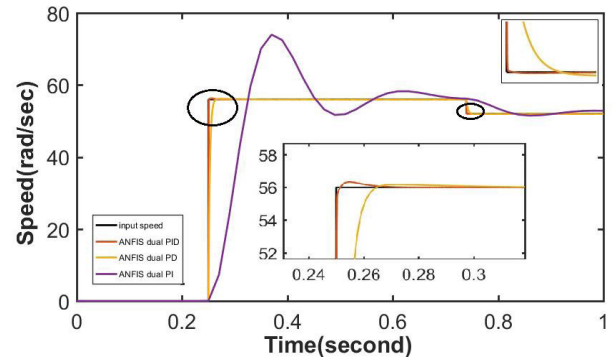


FIGURE 21. Speed sudden change response using ANFIS based  $PI_2$  and  $PD_2$ .

controller was performed to generate data for training ANFIS to solve the problem of the response speed. The data generated was too large; thus, it was reduced to the least possible amount to increase the controller speed response, which subsequently resulted in high performance. The results of the controller response using ANFIS based dual PID controller was illustrated in figure 19. The transient parameters of the ANFIS based dual PID controller was listed in table 5 and figure 22. For the designing of the ANFIS based dual PI controller, the controller showed varied response for speed (figure 19). As it is apparent in the figures, the ANFIS based dual PI controller showed better settling time and rise time than the ANFIS based  $PI_1$  controller, but simultaneously gained significant overshoot and oscillations.



**TABLE 5. The transient characteristics of the proposed controllers.**

The controller	Rise time (second)	Settling time(second)	Overshoot %
ANFIS-PI <sub>1</sub>	0.474	0.809	0.609
ANFIS-PD <sub>1</sub>	0.00966	0.0162	0.562
ANFIS-PID <sub>1</sub>	0.587	2.31	2.75
ANFIS-PI <sub>2</sub>	4.16	13.5	0
ANFIS-PD <sub>2</sub>	1.92	3.46	0
ANIF-PID <sub>2</sub>	1.66	6.08	7.77
ANFIS-dual PI	0.1.6	0.385	12.1
ANFIS-dual PD	0.00573	0.00984	0.376
ANFIS-dual PID	0.000107	0.000209	0

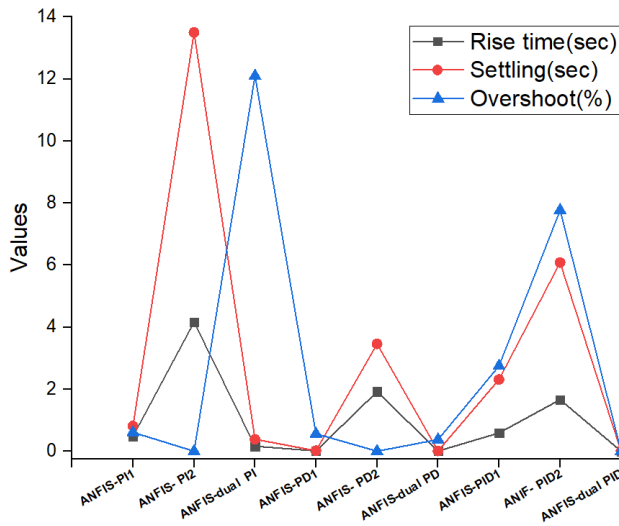


**FIGURE 22. The transient characteristics of the proposed controllers.**

Furthermore, any attempts to decrease the overshoot resulted to an increase in the rise time and settling time. Therefore, the option of a dual PI controller should be ignored if the overshoot is not an important factor. As evident in table 5 and figure 19, ANFIS based dual PD controller shows an improvement in all transient response aspects. Figure 20 shows the superiority of the ANFIS based dual PID and PD at time 0.1 seconds. The ANFIS based dual PID and PD were operated under sudden change of the speed, where the speed at time 0.25 second rose up to 56 rad/sec, and slowed down to 52 rad/sec at time 0.74, proving the efficiency of the controllers (Figure 21). ANFIS based dual PID showed optimal performance in all aspects.

**V. CONCLUSION**

This study evaluated the effect of the feed-forward data used to set ANFIS control by visualizing the DC motor speed behavior. For the training data for ANFIS controller, several models of PIDs were implemented and operated under various conditions to investigate the controllers’ performance. Based on Matlab Simulink tools, several characteristics were observed, such as steady-state error, the rise time, overshoot, and the settling time, which are all important in developing the dc’s motor performance. ANFIS showed simplicity in execution and learning susceptibility. Furthermore, the

implementation of the rules was easy compared to the retuning of the traditional control methods. The results demonstrated that ANFIS based dual PID has superior performance, high robustness, and excellent accuracy without oscillation for the speed control of the DC motor. The controller also showed high efficiency and distinct performance in tracking the motor speed compared to other suggested and previously studied controllers. The constraints of the method are that the performance of any pair of controllers is not equal, and the response of the conventional model used to generate data is too slow.

**REFERENCES**

- [1] R. Akkaya, A. A. Kulaksiz, and Ö. Aydoğdu, “DSP implementation of a PV system with GA-MLP-NN based MPPT controller supplying BLDC motor drive,” *Energy Convers. Manage.*, vol. 48, no. 1, pp. 210–218, Jan. 2007.
- [2] O. Aguilar-Mejía, R. Tapia-Olvera, A. Valderrabano-González, and I. R. Cambero, “Adaptive neural network control of chaos in permanent magnet synchronous motor,” *Intell. Automat. Soft Comput.*, vol. 22, no. 3, pp. 499–507, 2016.
- [3] M. Demirtas, “Off-line tuning of a PI speed controller for a permanent magnet brushless DC motor using DSP,” *Energy Convers. Manage.*, vol. 52, no. 1, pp. 264–273, Jan. 2011.
- [4] K. S. Alli, “A LabVIEW-based online DC servomechanism control experiments incorporating PID controller for students’ laboratory,” *Int. J. Elect. Eng. Educ.*, early access, Aug. 2019, doi: 10.1177/0020720919868142.
- [5] S. Peicheng, W. Suo, Z. Rongyun, and X. Ping, “Study on the fuzzy proportional–integral–derivative direct torque control strategy without flux linkage observation for brushless direct current motors,” *Int. J. Adv. Robotic Syst.*, vol. 16, no. 3, 2019, Art. no. 1729881419853141.
- [6] H. Hu, T. Wang, S. Zhao, and C. Wang, “Speed control of brushless direct current motor using a genetic algorithm–optimized fuzzy proportional integral differential controller,” *Adv. Mech. Eng.*, vol. 11, no. 11, 2019, Art. no. 1687814019890199.
- [7] B. Hekimoglu, “Optimal tuning of fractional order PID controller for DC motor speed control via chaotic atom search optimization algorithm,” *IEEE Access*, vol. 7, pp. 38100–38114, 2019.
- [8] J. Agarwal, G. Parmar, R. Gupta, and A. Sikander, “Analysis of grey wolf optimizer based fractional order PID controller in speed control of DC motor,” *Microssyst. Technol.*, vol. 24, no. 12, pp. 4997–5006, Dec. 2018.
- [9] D. Puangdownreong, “Optimal PID controller design for DC motor speed control system with tracking and regulating constrained optimization via cuckoo search,” *J. Elect. Eng. Technol.*, vol. 13, no. 1, pp. 460–467, 2018, doi: 10.5370/JEET.2018.13.1.460.
- [10] C.-H. Kim, “Multi-loop PID control method of brushless DC motors via convex combination method,” *J. Electr. Eng. Technol.*, vol. 12, no. 1, pp. 72–77, Jan. 2017.
- [11] A. R. Sartorius, J. de Jesus Moreno, O. Pinon, and A. E. Ruiz, “A new approach for adjusting scale factor in fuzzy PD+ I controllers with anti-windup,” *J. Intell. Fuzzy Syst.*, vol. 27, no. 5, pp. 2319–2326, 2014.
- [12] H.-P. Wang and Y.-T. Liu, “Integrated design of speed-sensorless and adaptive speed controller for a brushless DC motor,” *IEEE Trans. Power Electron.*, vol. 21, no. 2, pp. 518–523, Mar. 2006.
- [13] K. Premkumar and B. V. Manikandan, “Fuzzy PID supervised online ANFIS based speed controller for brushless DC motor,” *Neurocomputing*, vol. 157, pp. 76–90, Jun. 2015.
- [14] P. Tripura and Y. S. K. Babu, “Intelligent speed control of DC motor using ANFIS,” *J. Intell. Fuzzy Syst.*, vol. 26, no. 1, pp. 223–227, 2014.
- [15] K. Premkumar and B. V. Manikandan, “GA-PSO optimized online ANFIS based speed controller for brushless DC motor,” *J. Intell. Fuzzy Syst.*, vol. 28, no. 6, pp. 2839–2850, Aug. 2015.
- [16] M. John Prabu, P. Poongodi, and K. Premkumar, “Fuzzy supervised online coactive neuro-fuzzy inference system-based rotor position control of brushless DC motor,” *IET Power Electron.*, vol. 9, no. 11, pp. 2229–2239, Sep. 2016.
- [17] K. Navaneethakannan and M. Sudha, “Analysis and implementation of ANFIS-based rotor position controller for BLDC motors,” *J. Power Electron.*, vol. 16, no. 2, pp. 564–571, Mar. 2016.

- [18] T. S. Sivarani, S. J. Jawhar, C. A. Kumar, and K. P. Kumar, "Novel bacterial foraging-based ANFIS for speed control of matrix converter-fed industrial BLDC motors operated under low speed and high torque," *Neural Comput. Appl.*, vol. 29, no. 12, pp. 1411–1434, Jun. 2018.
- [19] G. Yanling and M. E. A. Mohamed, "Study on the extent of the impact of data set type on the performance of ANFIS for controlling the speed of DC motor," *J. Eng. Technol. Sci.*, vol. 51, no. 1, pp. 83–102, 2019.
- [20] H. Arpacı and O. F. Ozguven, "Design of adaptive fractional-order PID controller to enhance robustness by means of adaptive network fuzzy inference system," *Int. J. Fuzzy Syst.*, vol. 19, no. 4, pp. 1118–1131, Aug. 2017.
- [21] H. Suryoatmojo, M. Ridwan, D. C. Riawan, E. Setijadi, and R. Mardiyanto, "Hybrid particle swarm optimization and recursive least square estimation based ANFIS multioutput for BLDC motor speed controller," *Int. J. Innov. Comput., Inf. Control*, vol. 15, no. 3, pp. 939–954, 2019.
- [22] A. A. Hepzibah and K. Premkumar, "ANFIS current-voltage controlled MPPT algorithm for solar powered brushless DC motor based water pump," *Elect. Eng.*, vol. 102, pp. 421–435, Nov. 2019.
- [23] M. R. Faioghi and S. M. Azimi, "Design an optimized PID controller for brushless DC motor by using PSO and based on NARMAX identified model with ANFIS," in *Proc. 12th Int. Conf. Comput. Modeling Simulation*, 2010, pp. 16–21.
- [24] H. Bevrani and S. Shokoohi, "An intelligent droop control for simultaneous voltage and frequency regulation in islanded microgrids," *IEEE Trans. Smart Grid*, vol. 4, no. 3, pp. 1505–1513, Sep. 2013.
- [25] S. S. Chong, A. A. B. A. Raman, S. W. Harun, and H. Arof, "Dye concentrations measurement using Mach-Zehner interferometer sensor and modeled by ANFIS," *IEEE Sensors J.*, vol. 16, no. 22, pp. 8044–8050, Nov. 2016.
- [26] A. Senthilkumar and P. Ajay-D-Vimal Raj, "ANFIS and MRAS-PI controllers based adaptive-UPQC for power quality enhancement application," *Electr. Power Syst. Res.*, vol. 126, pp. 1–11, Sep. 2015.
- [27] K. Premkumar and B. V. Manikandan, "Adaptive neuro-fuzzy inference system based speed controller for brushless DC motor," *Neurocomputing*, vol. 138, pp. 260–270, Aug. 2014.



**YANLING GUO** received the bachelor's degree from the Department of Machinery, Dalian Institute of Technology under the supervision of Assoc. Prof. J. Xiuying, in July 1984, the master's degree from the Department of Mechanical Manufacturing and Automation, Harbin University of Technology under the supervision of Prof. L. Jipei, in January 1990, and the Ph.D. degree from the Department of Machinery Manufacturing and Automation, Harbin University of Technology under the supervision of Prof. Z. Wansheng, in March 2001.

She was a Professor and a Ph.D. Supervisor in mechanical and electronic engineering with the School of Mechanical and Electrical Engineering, Northeast Forestry University, Harbin, China. From September 1985 to August 1990, she held an Assistant position with the Department of machinery, Northeast Forestry College. She was a Lecturer, from September 1990 to September 1996 and from September 1996 to August 2003, she was an

Associate Professor and the master's Guide with the School of Mechanical and Electrical Engineering, Northeast Forestry University, where she has also been a Professor, since September 2003, and a Ph.D. Supervisor, since September 2004. From December 2008 to December 2009, she was a Visiting Scholar with the Wu Xianming Manufacturing Technology Center, University of Michigan, USA, under the supervision of Prof. N. Jun. From September 2001 to December 2003, she held a postdoctoral position with the Postdoctoral Mobile Station of Mechanical Engineering/Postdoctoral Workstation, Harbin Huawei Group, Harbin University of Technology, under the supervision of Prof. Z. Wansheng. She is currently a Ph.D. Supervisor, a First-Class Discipline Leader of mechanical engineering, and the Director of 3D Printing Materials and Technology Research and Development Center, Northeast Forestry University. She has presided over more than 20 projects of NSFC and published more than 150 articles. She holds eight authorized invention patents and 30 utility models. She has presided over four provincial teaching reform projects. In the research and development of new 3D printing equipment and CNC system of special machine tools, she has many research results. It is proposed that biomass composite materials are used as 3D printing consumables, which are successfully used in laser sintering additive manufacturing raw materials. It is called the fourth kind of additive manufacturing materials besides metal, inorganic non-metal, and polymer materials by the industry, domestic, and foreign media.

Dr. Guo is a Standing Member of the China Electrical Processing Society/Deputy Director of the International Exchange Committee, the Director of the China Association of popular science writers, and the Standing Director of the Material Committee of World 3D Printing Association. She received three provincial awards as the First Adult.



**MOHAMED ELHAJ AHMED MOHAMED** (Member, IEEE) received the B.S. degree in computer engineering from the Technologic and Science University, Khartoum, Sudan, in 2002, and the M.S. degree in computer and network engineering from the Department of Electrical Engineering, University of Khartoum, Sudan, in 2007. He is currently pursuing the Ph.D. degree in mechatronics engineering with the School of Mechanical and Electrical Engineering, Northeast

Forestry University, Harbin, China.

From 2002 to 2006, he was an Assistant Teacher and the Labs Director with the University of Karary, Khartoum. From 2006 to 2014, he was a Lecturer with the Department of Electrical and Electronic Engineering, University of Karary. He has published a few articles in developing dc motor control and electrical vehicles motor control. His research interests include development of control of dc motor and applying intelligent control techniques using developed special algorithms.

Mr. Mohamed received the China Government Scholarship and the Award from the Best Performance in Chinese Language.

...